

The Optimal Design of Fractional-slot SPM to Reduce Cogging Torque and Vibration

Gyu-Won Cho*, Woo-Sung Jang**, Ki-Bong Jang* and Gyu-Tak Kim†

Abstract – This paper deals with the analysis of vibration and noise sources in a modular-type SPM fractional-slot motor. To reduce cogging torque, torque ripple and unequal radial force, which are the main causes of the electromagnetic vibration, the optimal shape of notch and magnet are designed.

Keywords: SPMSM, Fractional slot, Modal analysis, Radial magnetic force

1. Introduction

This paper proposes a Permanent Magnet Synchronous Motor (PMSM) with concentrated winding whose field magnet flux does not rely on external power but is supplied by a permanent magnet of the rotor. The length of the end turn, which causes copper loss, is shorter. So, the efficiency and power density are much higher than those for other motors [1, 2].

Recently, a new topology for fractional-slot motors, often referred to as “modular-type”, has emerged [3]. This type of permanent magnet fractional-slot motor has a different winding layout compared with that of a conventional permanent magnet motor. Fig. 1 shows a winding layout of a modular-type Surface-mounted Permanent Magnet (SPM) fractional-slot motor of which pole to Slot Ratio is 5:6.

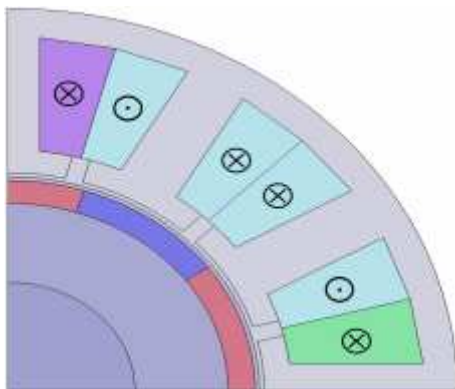


Fig. 1 Winding layout

The back-EMF waveform of this ring-type multi-pole magnet motor is significantly more sinusoidal than that of

the conventional permanent magnet motor because the fifth and seventh harmonics are much smaller. Also, the cogging torque is smaller than that of the conventional permanent magnet motor since motor has a great number of least common multiples of slots and poles. For these reasons, the modular-type SPM fractional-slot motor has a higher torque density and lower torque ripple.

However, the magnetic field of this type of winding has more space harmonics, which cause noise and vibration; this vibration is the greatest weakness of the modular-type motor. And, unequal radial magnetic force in the air gap is the main cause of electromagnetic vibration. In this paper, in order to reduce cogging torque and torque ripple, an optimal notch is designed and the radial magnetic force is analyzed; then, an optimal magnet shape is designed for equal distribution of radial force.

2. Magnetic Circuit Design for Vibration Reduction

2.1 Modal analysis

All resonance frequencies and all possible deformations of the structure can be computed with the modal analysis, which depends only on the design parameters and the material properties. Free vibration is generated by inherent forces in the absence of external forces. The field has one or more the natural frequencies in case of free vibration. The natural frequencies are determined by the distribution of mass and stiffness and it is the unique characteristics of a dynamic system. Finite Element Method(FEM) is used for the free vibration analysis; the vibration equation for an undamped system is as in the following equation [4].

$$[\mathbf{M}]\{\ddot{x}\} + [\mathbf{K}]\{x\} = 0 \quad (1)$$

where $[M]$ and $[K]$ are the global mass matrix and stiffness matrix, respectively. $\{\ddot{x}\}$ and $\{x\}$ are the acceleration and the displacement at each point of the

† Corresponding Author: Dept. of Electrical and Electronic Engineering, Changwon National University, Korea. (gtkim@Changwon.ac.kr)

* Dept. of Electrical and Electronic Engineering, Changwon National University, Korea.

** Dept. of Research Engineer / W/M Control HA Control R&D Lab. LG Electronics Inc, Korea. (woosung12.jang@lge.com)

Received: December 19, 2011; Accepted: June 13, 2012

system. For a linear system, a solution of the free vibration will be harmonic in form, as in the following equation.

$$\{x(t)\} = \{\Phi\}_i e^{i\omega_i t} \quad (2)$$

ω_i is the i^{th} natural frequency, $\{\Phi\}_i$ is an eigenvector representing the mode shape of the i^{th} natural frequency and t is the time. Substituting (2) in (1), it can be rewritten as following.

$$([\mathbf{K}] - \omega_i^2 [\mathbf{M}])\{\Phi\}_i e^{i\omega_i t} = 0 \quad (3)$$

$$([\mathbf{K}] - \omega_i^2 [\mathbf{M}]) = 0 \quad (4)$$

This equation is the eigenvalue problem and represents the natural frequencies of the system; the natural frequencies occur in the same number as the free vibration. To investigate the natural frequencies and mode shapes, only the stator is considered. Material constants needed for the analysis are assumed to be homogeneous and isotropic and lamination of the stator is not considered. Mode shows that unique dynamic aspect in the vibration systems. With the force of the stator in a frequency band with a unique mode appears as a pattern when the stator is vibrated by excited force. Vibration modes of the stator can be divided into three parts. Firstly, circumferential mode with two-dimensional planar motion in the axial direction of the change is constant. Secondly, the longitudinal mode in the direction of the laminate is to have periodic variations. Lastly, the radial mode is defined by the circumference mode and axial modes are different of vibration shape.

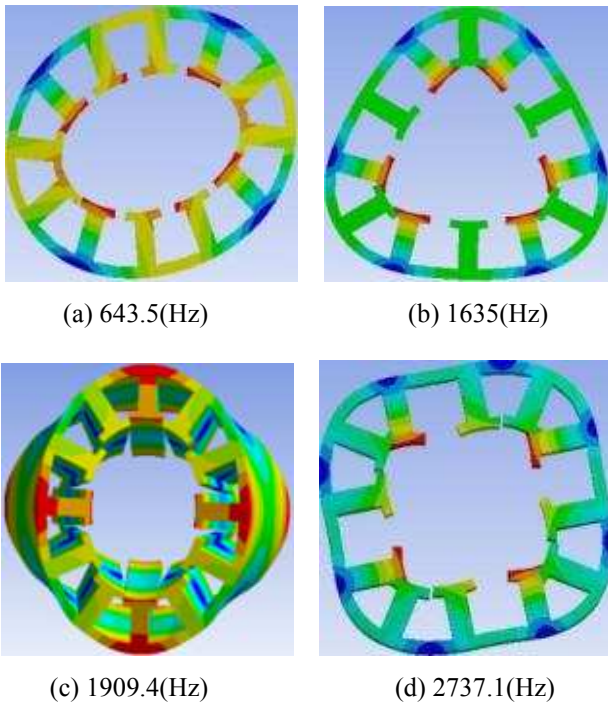


Fig. 2 Mode shapes corresponding to natural frequencies

Fig. 2 shows mode shapes corresponding to natural frequencies. Fig. 2(a) and (c) are the oval modes at 643.5(Hz) and 1909.4(Hz), respectively. These modes are the main components of the vibration and noise, so the resonance in this mode should be avoided.

2.2 Reduction of vibration by cogging torque reduction

Sources of vibration in the motor can be divided by mechanical and electromagnetic vibration. Firstly, Sources of mechanical vibration have rotor dynamic, rotor unbalance, bearings, flexible shaft etcetera. Secondly, Sources of electromagnetic vibrations have the cogging torque, torque ripple, and time-varying traction. Lastly, the main reason is radial force which is a force between rotor and stator in excited force. So, it makes vibration and noise. In particular, if oscillation frequency of the electromagnetic excited force is similar to oscillation frequency of the motor structure, motor have not only abrasion of component but also performance degradation of motor. So, it is necessary to minimize vibration and noise for excited force.

The cogging torque is an irregular torque in the motor and the force of the tangential direction that moves to a location where the magnetic energy is minimal. Regardless of the load current, the cogging torque is caused by the interaction between the permanent magnet and the slot. For the IPMSM, the cogging torque is largely generated due to a considerable change in the magnetic distribution on the rotor surface including a permanent magnet. The position (α) and width (γ) of the notch, which can offset the cogging torque, can be calculated with the energy distribution of the air-gap using a Fourier Series, because the cogging torque is generated by the irregular magnetic distribution on the rotor surface. For the slotless IPMSM, which changes a permeance in the air-gap, the energy function according to the magnetization distribution is as shown in Fig. 3.

$$f(\phi) = \frac{B_i^2(\phi)}{2\mu_0} = X_0 + \sum_{k=1}^{\infty} X_k \sin(kP\phi + \frac{\pi}{2}). \quad (5)$$

The cogging torque is presented as a harmonic wave during the motor operating, and it is multiples dividing the least common multiple of the number of permanent magnet poles and slots by poles. Therefore, the frequency of cogging torque formula is as follows:

$$f_{Pn} = \frac{nG}{P} = \frac{nLCM(S,P)}{P}, \quad n = 1, 2, 3, \dots \quad (6)$$

In order to reduce the cogging torque of the harmonic components shown as the above formula, a notch that can change the distribution of the flux density shape is designed.

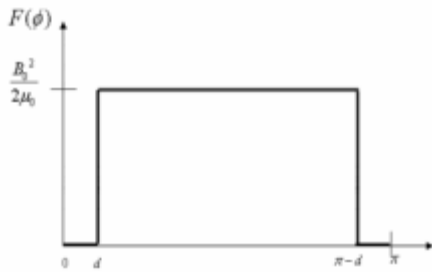


Fig. 3. The equivalent magnetization distribution of the basic model.

That is, a torque that is opposite the cogging torque is generated by changing the flux density of the air-gap. Thus, the cogging torque is offset. Fig. 4 shows the equivalent magnetization distribution of the notch applied model [6].

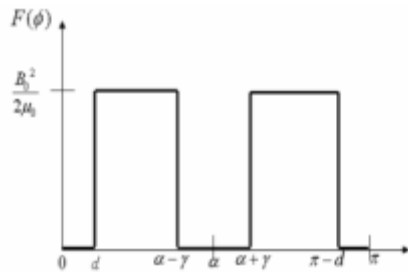


Fig. 4. The equivalent magnetization distribution of the notch applied model.

In the PMSM, a magnetic force always exists between the permanent magnet and the stator core. This force, along with the impact of the torque, produces cogging torque by the mutual attraction between teeth of the stator and the permanent magnet that is installed in the rotor. In the permanent magnet motor, the cogging torque is the main source of the vibration; the frequency of the cogging torque that is affected by the least common multiple of slots and poles is as follows.

$$f_c = k \times l_{cm} \times \frac{N_s}{60} \tag{7}$$

where f_c is the frequency of the cogging torque, k is an integer (1,2,3,...), l_{cm} is the least common multiple of slots and poles, and N_s is the revolutions per minute. The magnitude of the cogging torque is decided by the radial flux density B_r and the tangential flux density B_t , as shown in (8).

$$T_{cog}(t) = \frac{L_{ef} \cdot r^2}{\mu_0} \int_0^{2\pi} B_r B_t d\phi \tag{8}$$

$$\frac{1}{\mu_0} B_r B_t = \text{circumferential stress}$$

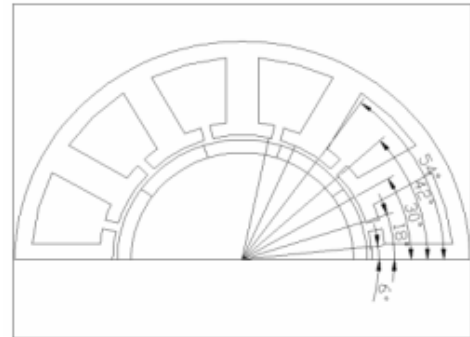
where L_{ef} is the effective stack length, r is the radius of the flux density as calculated and μ_0 is the permeability of air.

In order to reduce the cogging torque, the functions of cogging torque and dummy slot are found using a Fourier series and then notch design parameters are decided. Finally, the function of the notch design is as follows.

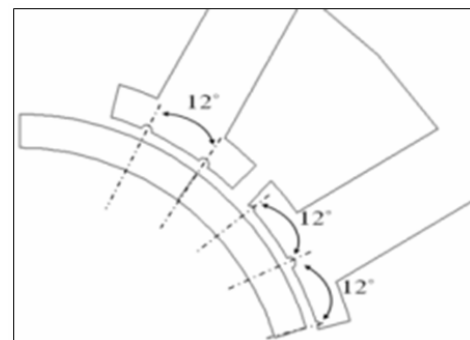
$$\cos(f_{pn}\theta) + \frac{\sin(f_{pn}r)}{\sin(f_{pn}a)} \cdot \cos(f_{pn}(\theta+x)) = 0 \tag{9}$$

$$f_{pn} = \frac{nLCM(S,P)}{P}, \quad n = 1, 2, 3, \dots$$

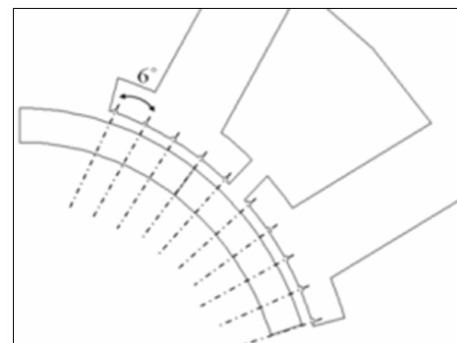
where n is the degree of the harmonics, r is the width of the dummy slot and x is the position of the dummy slot. The position and width of the notch are shown in Fig. 5.



(a) positions of notches



(b) notch 1

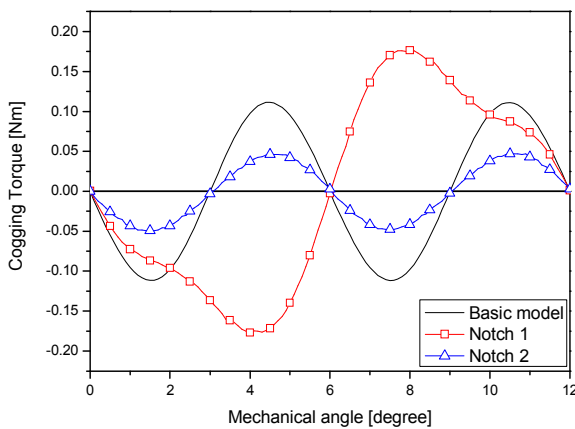


(c) notch 2

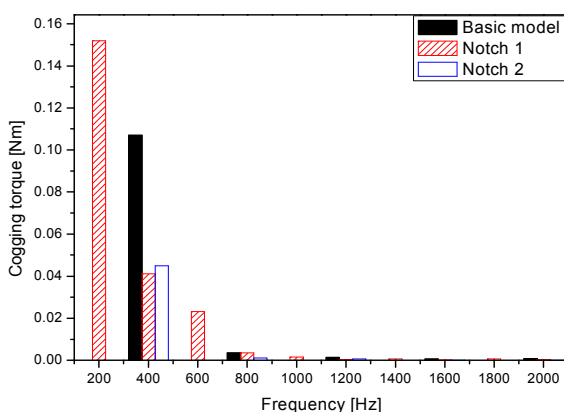
Fig. 5. Position and width of notches

In the case of the Notch 1 model, the position and width of the notch are found using a Fourier series. As shown in Fig. 5(b), in the case of the modular-type SPM fractional-slot motor, when the positions of the notch are found by Fourier series, it can be seen that the positions of the notch are not distributed on all of the teeth equally, which is different from the situation of the conventional permanent magnet motor. Fig. 6 shows the cogging torques and time harmonic distributions of the basic model and the notch models. It can also be ascertained that the frequency components of the cogging torque, found with Eq. (7), coincide with the analysis value.

In the case of the Notch 1 model, as shown Fig. 6, it can be seen that the fundamental harmonic of the cogging torque increases by 42.1(%) compared with that of the basic model, which causes an increment of torque ripple. Also, it is predicted that the amplitude of vibration is larger than that of the basic model because 600(Hz) component of cogging torque and mode (a) of natural frequency resonate.



(a) cogging torque



(b) time harmonic distribution

Fig. 6. Characteristic of cogging torque

However, in the case of the notch 2 model, the fundamental harmonic of the cogging torque decreases by 57.9(%) compared with that of the basic model, which

causes a decrease of torque ripple. No resonances were occurred between frequencies of cogging torque and natural frequencies.

2.3 Reduction of vibration by equal distribution of radial force

The radial force density distribution on the stator surface, which results from the air-gap magnetic field under no-load and on-load conditions, is the main cause of electromagnetic noise and vibration, and can be evaluated analytically by Maxwell's stress tensor method [5, 7]. Thus,

$$F_{rad}(\theta_s, t) = \frac{1}{2\mu_0} [B_r^2(\theta_s, t) - B_\theta^2(\theta_s, t)] \quad (10)$$

where F_{rad} is the radial component of force density, B_r and B_θ are the radial and tangential components of the air-gap flux density, μ_0 is the permeability of free space, θ_s is the angular position at the stator and t is the time. The radial force density of the basic model, using (10), is shown in Fig. 7. The black line means radial force density and red line is radial force density distribution. In the case of the basic model, the distribution of the radial force density is close to oval-shaped, so it is predicted that the amplitude of vibration will be larger than that of the conventional permanent magnet motor.

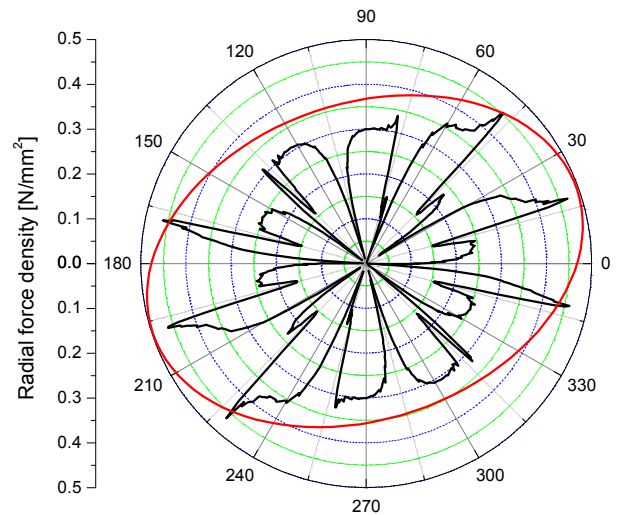


Fig. 7. Radial force density of the basic model

So it is necessary to eliminate the harmonics of the air gap flux density by equal radial force density distribution; resonances between the frequencies of the radial force density and the natural frequencies of the stator should be avoided. The frequency spectrum of the radial force density is shown in Fig. 8. It is confirmed that the amplitudes of the frequency bandwidth of the resonance possibility are very small compared to the major components of radial force density. Therefore, it is

considered that the effect of resonance can be disregarded, compared with the frequency components of each mode in Fig. 2.

The harmonics in the air gap flux density due to the magnet field and armature reaction field are shown in Fig. 9. It is confirmed that the magnet field includes harmonics orders 5th, 15th, 25th, ..., while the armature reaction field includes 1st, 5th, 7th, 11th, 13th, The interaction between the odd space harmonics in the magnetic field and the armature reaction field has a major effect on the radial force density.

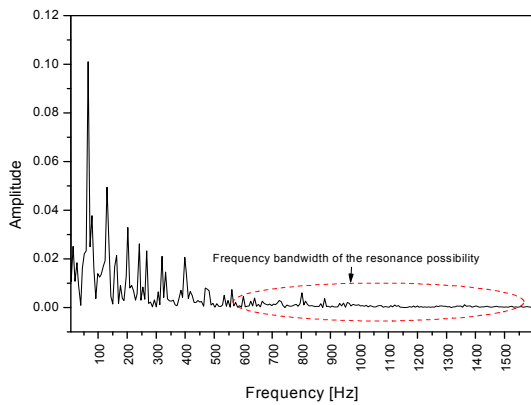
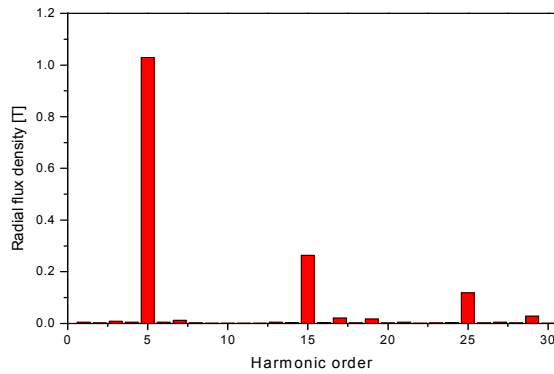
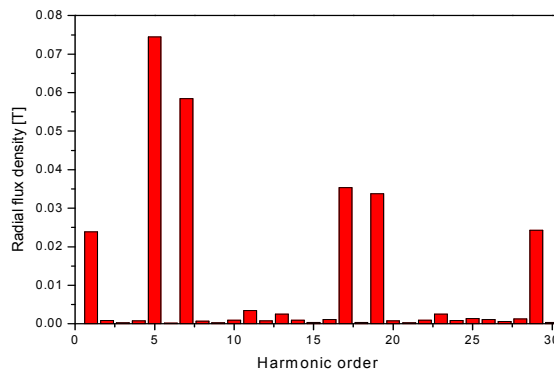


Fig. 8. Frequency spectrum of the radial force density



(a) magnet field



(b) armature reaction field

Fig. 9. Harmonics in air gap flux density

To distribute radial force density equally, the optimal design of the magnet shape and dummy slot was carried out as shown in Fig. 10. FEM and DOE (Design of Experiment) were used for optimal design of the magnet shape. Design parameters A, B, and C are 13.75 (mm), 23.98(mm) and 13.75(mm), respectively. In the case of the proposed model, the harmonic components of the radial force density mostly decreased, except for the 10th harmonic of radial force density, compared with those of the basic model shown in Fig. 11.

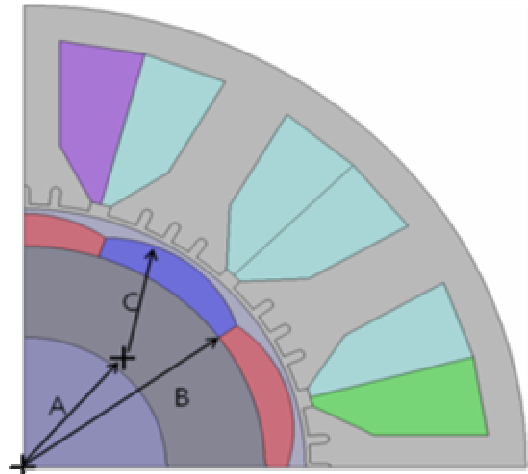


Fig. 10. Proposed model

The radial force density of the proposed model is shown in Fig. 12. Due to the equal distribution of the radial force density, it is predicted that the electromagnetic vibration will be reduced.

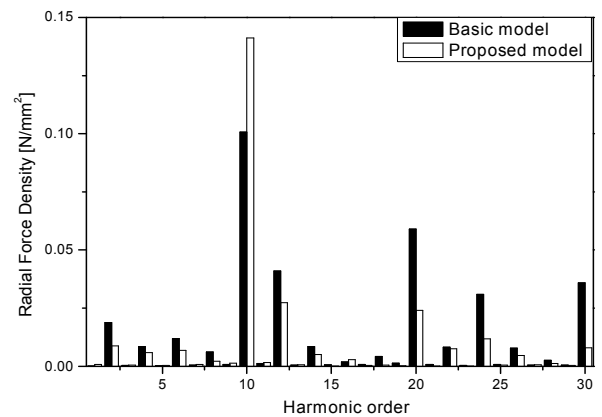


Fig. 11. Harmonic analysis of Radial force density

However, because the effective air-gap length in this model is a little larger than that of the basic model, the average output torque of the proposed model is slightly smaller than that of the basic model, as shown in Fig. 13. Nevertheless, in the case of the proposed model, the torque ripple is considerably improved to 1.16(%), compared with that of the basic model, which is 6.18 (%).

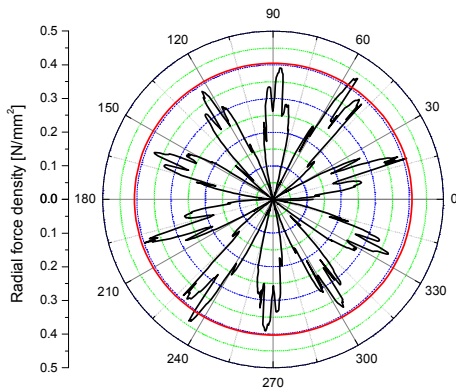


Fig. 12. Radial force density of the proposed model

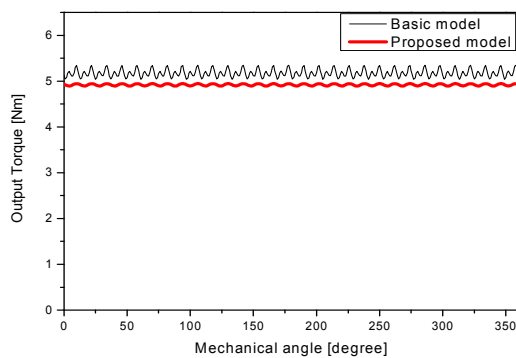


Fig. 13. Comparison of output torques

3. Conclusion

This study deals with the analysis of vibration sources and method of vibration reduction in a modular-type SPM fractional-slot motor. By applying a new-type of notch and optimal design of the magnet, it is expected that the amplitude of vibration electromagnetic vibration will be reduced as a result of decreased cogging torque and equal distribution of radial force density. Later, a prototype machine will be made and then a comparison of experimental and analyzed values will be done to prove the validity of this research.

Acknowledgements

This research was financially supported by the MEST and NRF through the Human Resource Training Project for Regional Innovation and the Second Stage of Brain Korea21 Projects.

References

- [1] C.C. Chan, J. Z. Jiang, G. H. Chen, X. Y. Wang, and K. T. Chau, "A novel polyphase multi-pole square-wave permanent magnet motor drive for electric vehicles", *IEEE Trans. on Industry Applications*, vol. 30, no. 5, pp.1258-1266, 1994.
- [2] J. Cros and P. Viarouge, "Synthesis of high performance PM motors with concentrated windings", *IEEE Trans. on Energy Conversion*, vol. 17, no. 2, pp. 248-253, 2002.
- [3] Atallah, K., Wang, J and Howe, D., "Torque ripple minimization in modular permanent magnet brushless machines," *IEEE Trans. on Industry Application.*, vol. 39, no. 6, pp. 1689-1695, 2003.
- [4] Logan, Daryl L., "A First Course in the Finite Element Method", Thomson Learning, 2007
- [5] Gieras, J. F.; Wang, C.; Lai, J. C.; "Noise of Polyphase Electrical Motors", Taylor & Francis Group, 2006
- [6] G.H.Kang, Y.D.Son, G.T.Kim, J.H.Hur, "A Novel Cogging Torque Reduction Method for Interior-Type Permanent-Magnet Motor", *IEEE Trans. on Industry Application.*, vol. 45, no. 1, pp. 161-167, 2009.
- [7] M.N.Anwar, I.Husain, "Radial Force Calculation and Acoustic Noise Prediction in Switched Reluctance Machines", *IEEE Trans. on Industry Application.*, vol. 36, no. 6, pp. 1589-1579, 2000.



Gyu-Won Cho He received B.S and M.S degree in electrical engineering from Changwon National University, Korea. He is currently pursuing his Ph.D. degree at Changwon National University. His research interests are electrical machine and FEM analysis.



Woo-Sung Jang He received M.S degree in electrical engineering from Changwon National university, Korea. His research interests are electrical machine and FEM analysis.



Ki-Bong Jang He received B.S, M.S and Ph.D degree in electrical engineering from Hanyang University, Korea. He is presently a Professor of Changwon National University. His research interests are electrical machine and FEM analysis.



Gyu-Tak Kim He received B.S, M.S and Ph.D degree in electrical engineering from Hanyang University, Korea. He is presently a Professor of Changwon National University. His research interests are electrical machine and FEM analysis.